Analyst

Accepted Manuscript

This article can be cited before page numbers have been issued, to do this please use: A. Boujakhrout, S. Jimenez, P. Martínez-Ruiz, A. Sánchez, P. Díez, J. M. Pingarron and R. Villalonga, *Analyst*, 2016, DOI: 10.1039/C5AN02640G.

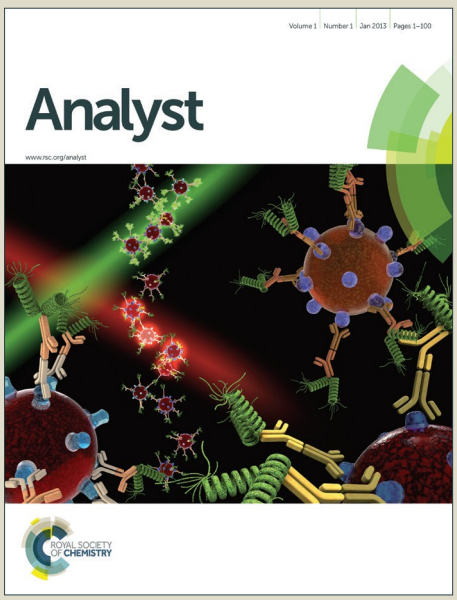

ROYAL SOCIETY OF CHEMISTRY

www.rsc.org/analyst

Dynamic Article Links ▶
View Article Online
DOI: 10.1039/C5AN02640G

Cite this: DOI: 10.1039/c0xx00000x

www.rsc.org/xxxxxx

ARTICLE TYPE

Novel reduced graphene oxide-glycol chitosan nanohybrid for the assembly of amperometric enzyme biosensor for phenols

Abderrahmane Boujakhrout,[a] Sandra Jimenez-Falcao,[a] Paloma Martínez-Ruiz,[b] Alfredo Sánchez,[a] Paula Díez,[a] José M. Pingarrón,*[a,c] Reynaldo Villalonga*[a,c]

Received (in XXX, XXX) Xth XXXXXXXXX 20XX, Accepted Xth XXXXXXXXX 20XX
DOI: 10.1039/b000000x

A novel water-soluble graphene derivative was prepared from graphene oxide through a two-step modification approach. Graphene oxide was first provided with reactive epoxy groups by covalent modification with (3-glycidyloxypropyl)trimethoxysilane and further cross-linked with glycol chitosan. This graphene derivative was characterized by different microscopy and physicochemical methods and employed as coating material for glassy carbon electrode. The nanostructured surface was used as support for the covalent immobilization of the enzyme laccase through cross-linking with glutaraldehyde. The enzyme electrode was tested for the amperometric detection of different phenolic compounds, showing excellent analytical behaviour toward catechol with a linear range of response from 200 nM to 15 µM, sensitivity of 93 mA/M cm^2, and low detection limit of 76 nM. The enzyme biosensor showed high stability when stored at 4ºC under dry conditions, and was successfully employed to quantify total phenolic compounds in commercial herbal tea samples.

Introduction

The design of reliable, highly sensitive, reproducible and selective electrochemical biosensors implies the preparation of advanced 3D transducer elements with specific chemical functionalities allowing high loadings and stable immobilization of bioreceptors. These transducer interfaces should also provide proper hydrophilic microenvironments for the successful occurrence of the biorecognition process.[1-3] In addition, they should have high electroconductive properties to ensure fast electron transfer at the sensing surface.[4,5]

During last decades, nanomaterials engineering has provided a great variety of advanced electroconductive materials with well-defined morphology, size and composition, able to be used as building blocks for the assembly of novel 3D transducer elements.[4-8] In this context, special interest has been devoted to prepare new graphene-based nanomaterials for electrochemical biosensing[9-12] due to the relative low cost, large surface-to-volume ratio and remarkable electrical, mechanical and thermal properties and biocompatibility of this nanomaterial.[13]

However, graphene nanosheets are highly hydrophobic materials consisting entirely of sp_2-hybridized carbon atoms without any other chemical functional groups.[14] This structural characteristic causes a very low solubility in water and does not allow stable and large immobilization of bioreceptors through covalent linkages.[15] That is why the development of new graphene-based composite and hybrid nanomaterials with tailored characteristics is a challenge for biosensor technology.

Recently, we proposed the covalent modification of silanized reduced graphene oxide derivatives with water-soluble polymers as a rational approach to prepare highly conductive nanomaterials enriched with hydrophilic chemical groups.[10,16-18] This synthetic strategy ensures preparation of highly functionalized graphene derivatives with low modification of its basal structure, then preserving the π-conjugated carbon-based structure.

It should be highlighted that chitosan, a linear amino polysaccharide of glucosamine and N-acetylglucosamine units obtained by alkaline deacetylation of chitin, has been largely employed to prepare graphene derivatives for biosensing purposes.[19-21] This fact has been supported by the unique polycationic and biocompatibility properties of this polymer.[19] However, low solubility of chitosan in neutral and alkaline media limits the preparation of full water-soluble graphene-based nanocomposite and nanohybrids.

In this work we describe for the first time the preparation of an original graphene nanohybrid, involving a water-soluble chitosan derivative, for its use as transducer element for electrochemical biosensing. For this purpose, GO was first modified with (3-glycidyloxypropyl)trimethoxysilane in order to provide the nanomaterial with highly reactive epoxy groups. This silanized derivative (Sil-GO) was further covalently grafted with glycol chitosan, a highly soluble chitosan derivative in a broad range of pH.[22] The resulting nanohybrid was employed as modifier for glassy carbon electrodes. Covalent immobilization of the enzyme laccase (Lac, EC 1.14.18.1) on this nanostructured surface allows the assembly of a reliable electrochemical biosensor for catechol and other phenols.

From an analytical point of view, the construction of new electrochemical biosensors for phenolic compounds has received considerable attention in last years[23-33] due to the increasing

View Article Online
DOI: 10.1039/C5AN02640G

evidence on the favourable health effects of (poly)phenol-rich foods on the prevention of cancers and many chronic illness such as cardiovascular disease or type II diabetes.[34,35] On the other hand, the sensitive determination of toxic phenolic endocrine disrupting compounds, such as catechol,[36] constitutes a priority in environmental analysis.

Materials and Methods

Materials

Laccase from *Trametes versicolor* (10 U/mg), (3-glycidyloxypropyl)trimethoxysilane, glycol chitosan (GC) and glutaraldehyde were acquired from Sigma-Aldrich Co. (USA). Graphene oxide was acquired from NanoInnova Technologies (Spain). All other chemicals were analytical grade.

Apparatus, electrodes and solutions

FT-IR spectra were acquired with a Nicolet Nexus 670/870 spectrometer (Thermo Fisher Scientific Inc., USA). Thermal analysis was performed with a TA Instruments SDT-Q600 apparatus (USA). Raman spectra were acquired with a Senterra dispersive micro Raman spectrometer (Bruker, USA). High resolution field emission scanning electron microscopy (FE-SEM) measurements were performed with a JEOL JSM-6335F microscope (JEOL Ltd., Japan). Transmission electron microscopy (TEM) measurements were performed with JEOL JEM-2000 FX microscope (JEOL Ltd., Japan).

Electrochemical impedance spectroscopy measurements were performed with a FRA2 µAutolab Type III potentiostat/ galvanostat, and the data was acquired using Frequency Response Analyser software (Metrohm Autolab B.V., The Netherlands). Amperometric measurements in stirred solutions at 300 rpm were carried out with a dual-channel ultrasensitive Inbea potentiostat (Inbea Biosensores S.L., Spain). A conventional three-electrode system was employed in the electrochemical studies, where the working electrode was a glassy carbon electrode (GCE, 3.0 mm diameter) modified with the graphene derivative and the immobilized enzyme. An Ag/AgCl/KCl (3 M) and a Pt wire were used as reference and counter electrodes, respectively. The measurements with the biosensor were carried out at 25ºC in 0.1 M sodium phosphate buffer, pH 6.0 (working volume 10 ml). 10µM and 100 µM cathecol solutions in 50 mM sodium phosphate buffer, pH 5.5, were freshly prepared.

Synthesis of GC-rGO

GO (50 mg) was dispersed in 250 mL ethanol by sonication during 1 h. The dispersion was then heated at 65ºC, mixed with 25 mL of a 1% (v/v) ethanolic solution of (3-glycidyloxypropyl) trimethoxysilane and kept under continuous stirring at this temperature during 12 h.[16] The mixture was cooled and filtered and the resulting solid (Sil-GO) was washed several times with ethanol and then dried in vacuum. The GC-rGO derivative was prepared by dispersing 50 mg Sil-GO in 100 mL double distilled water by sonication, and further mixed with 100 mL of a 1 mg/mL GC aqueous solution. The mixture was stirred at room temperature for 12 h, then filtered and the solid was washed several times with ethanol and finally dried under vacuum at room temperature.

Preparation of the enzyme electrode

A polished GCE was coated with the hybrid nanomaterial by depositing 25 µL of 0.5 mg/mL aqueous dispersion of GC-rGO on the electrode surface and allowing drying. Laccase was immobilized on the nanostructured electrode by dropping 20 µL of a 10 mg/mL enzyme solution in 100 mM sodium phosphate buffer, pH 5.5, and mixed with 2 µL of 25% (v/v) glutaraldehyde. The electrode was kept at 4ºC for 1 h, then washed several times with cold 50 mM sodium phosphate buffer, pH 5.5, and finally stored in refrigerator until use (Lac/GC-rGO/GCE). The amount of immobilized enzyme was estimated by Bradford protein assay.

Herbal tea samples preparation and measurements

Herbal tea samples (0.7 – 2.0 g, Lipton) were first weighted and further mixed with 100 mL boiled water. The mixtures were boiled during 10 min, then cooled at room temperatures and raised to 100 mL with double distilled water. Total phenol was determined by the Folin-Ciocalteau method according to the following procedure.[37] Double distilled water (2.0 mL), 200 µL herbal teas extract sample, 500 µL Folin-Ciocalteau reagent and 2.0 mL of 1.89 M Na_2CO_3 solution were sequentially added to 10.0 mL volumetric flasks. The mixtures were raised to 10.0 mL with water, homogenized and kept in the dark for 30 min. The absorbance at 750 nm was finally measured with a Varian Cary 3 UV-Visible spectrophotometer (Agilent Technologies, USA).

Results and discussion

Scheme 1 shows the two-steps synthesis of the GC-rGO nanohybrid, its use as coating material for GCE and the further covalent immobilization of laccase to construct the enzyme biosensor.

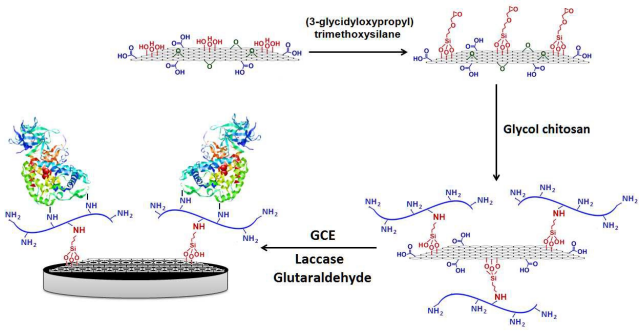

Scheme 1. Schematic display of the steps involved in the preparation of the GC-rGO hybrid nanomaterial and the enzyme electrode

The hybrid nanomaterial was prepared by treatment of GO with (3-glycidyloxypropyl)trimethoxysilane[16]. This treatment provoked the enrichment of GO basal plane with reactive epoxy groups which were further employed as anchoring points for the covalent cross-linking with glycol chitosan. Primary amino groups at the D-glucosamine moieties in the polysaccharide chains can form stable secondary amine linkages with the silane groups in Sil-GO through nucleophilic reactions. This reaction provoked the partial reduction of the oxygen functional groups at the basal plane of GO, thus forming the GC-reduced GO nanohybrid. Taking into account the high density of epoxy and amino groups in the reactant GO and glycol chitosan materials, it

View Article Online
DOI: 10.1039/C5AN02640G

is expected the formation of highly cross-linked derivatives. This was confirmed by FE-SEM and TEM analysis (Figure 1S in Supporting Information). As can be observed in Figure 1, GO deposited on GCE surface showed the classical extended sheet-like morphology, which was partially crumpled after covalent cross-linking with the cationic polysaccharide. These partially crumpled structures could be formed either by cross-linking a single GO sheet or by the association of several GO nanostructures into more complex polymer-based derivatives. Similar crumpled structures were previously described for GO cross-linked with polyamidoamine dendrimers.

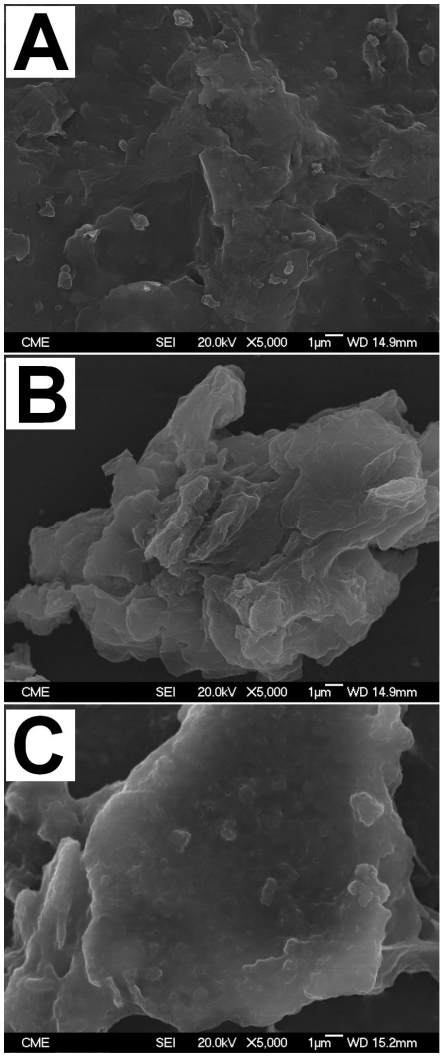

Figure 1. Representative FE-SEM images of GO/GCE (A), GC-rGO/GCE (B) and Lac/GC-rGO/GCE (C).

The resulting GC-rGO derivative was easily dispersed in double distilled water, yielding black dispersions that were stable for at least two weeks at room temperature. This fact could be ascribed to the presence of highly soluble glycol chitosan molecules in this derivative, increasing the hydrophilic character and the hydrodynamic volume of the GC-rGO adduct. In addition, the presence of hydrophilic oxygen groups at the basal plane and edges of GO should also contribute to the formation of stable aqueous dispersions from GC-rGO.

Graphene derivatives were characterized by FT-IR spectroscopy, and the corresponding spectra are shown in Figure 2A. GO exhibited the characteristics $\upsilon_{O\text{-}H(free)}$, $\upsilon_{O\text{-}H(associated)}$, $\upsilon_{C=O}$, $\upsilon_{C\text{-}OH}$, $\upsilon_{C\text{-}O\text{-}O}$ and $\upsilon_{C\text{-}O}$ stretching peaks at 3605 cm^{-1}, 3090 cm^{-1}, 1730 cm^{-1}, 1351 cm^{-1}, 1230 cm^{-1} and 1063 cm^{-1}, respectively.[16] The spectrum of Sil-GO derivative was characterized by the presence of peaks at 2880 cm^{-1} and 1412 cm^{-1}, which can be associated to the stretching and bending of the $–CH_2$ groups from the (3-glycidyloxypropyl)trimethoxysilane molecules, respectively. In addition, the presence of silane moieties in this derivative was confirmed by the characteristic $\upsilon_{Si\text{-}O\ (free)}$ stretching peak at 985 cm^{-1}.

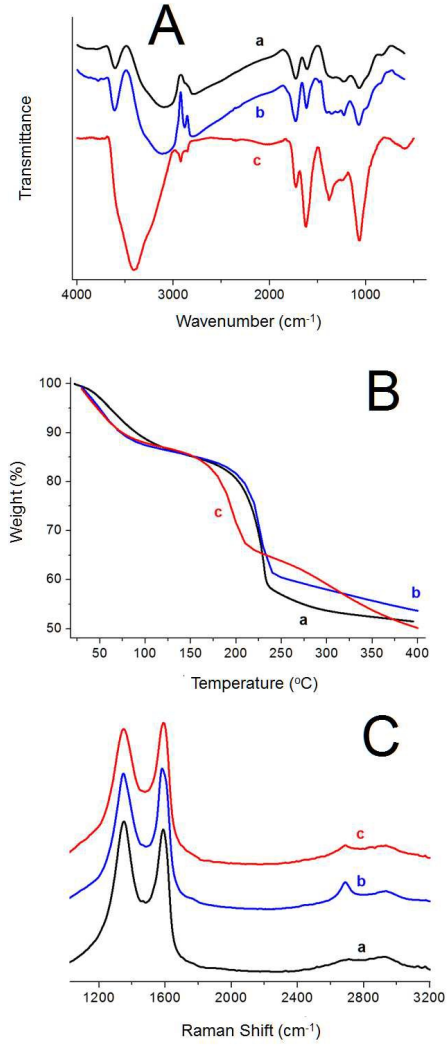

Figure 2. A) FT-IR, B) thermogravimetric analysis and C) Raman spectroscopy of GO (a), Sil-GO (b) and GC-rGO (c).

On the other hand, the presence of the cationic polysaccharide in the GC-rGO adduct was confirmed by the broad peak centred at 3400 cm^{-1}, corresponding to the stretching vibrations of the O-H and N-H groups, and the $\upsilon_{C\text{-}H}$ peak at 2915 cm^{-1}. In addition, the characteristics amide I and II peaks at 1726 cm^{-1} and 1623 cm^{-1}, respectively, confirmed the presence of N-acetylglucosamine residues in the GC-rGO derivatives. The relative broad peak at 1062 cm^{-1}, which is related to the stretching of the C-O-C groups in 6-member monosaccharide rings, also confirmed the

View Article Online
DOI: 10.1039/C5AN02640G

attachment of glycol chitosan to the GO sheets.

The thermal stability of the GO derivatives was studied by thermogravimetric analysis. The corresponding thermograms are shown in Figure 2B. GO experimented a first thermal transformation process in the range of 25-150ºC (ca. 14.1%) corresponding to the removal of residual water. A second thermal decomposition occurred at 200-250ºC (ca. 31.2%), which could be ascribed to the degradation of the oxygen functional groups at the edge and basal plane of the nanomaterial. Modification with (3-glycidyloxypropyl) trimethoxysilane slightly increased the thermal stability of the nanomaterial by shifting the temperature for the maximum rate of weight loss from 230ºC to 232ºC, also causing a noticeable reduction in the thermal weight loss of GO after this modification. As expected, cross-linking with glycol chitosan provoked a drastic reduction in the thermal stability of the hybrid nanomaterial, shifting the temperature for the maximum rate of thermal decomposition from 232ºC to 195ºC in comparison with the silanized derivative. A noticeable increase of 7% was observed for the thermal weight loss of GC-rGO, in comparison with Sil-GO. This difference remained the same up to 1000ºC (data not show), and accordingly, a polysaccharide content of 17.4% (as D-glucosamine) was estimated for the GC-rGO nanohybrid.

Figure 2C shows Raman spectra of the graphene oxide derivatives. The spectrum of GO showed broad G and D bands at 1584 cm^{-1} and 1344 cm^{-1}, which characterize the in-phase vibration of the graphite lattice and the structural disorders at the graphite edges, respectively. These bands were only slightly shifted to 1580 cm^{-1} and 1348 cm^{-1} and the D/G intensity ratio of 0.96 remained unchanged after modification with (3-glycidyloxypropyl)trimethoxysilane. However, the noticeable increase in the 2D band intensity at 2644 cm^{-1} suggests a partial restacking of the graphene nanosheets in the Sil-GO derivative. Further cross-linking with glycol chitosan caused a slightly shift in the G and D bands 1589 cm^{-1} and 1349 cm^{-1}, respectively, as well as a slight increase in the D/G intensity ratio to 0.98, suggesting a chemical interaction between the polysaccharide chains and the graphene sheets. In addition, the noticeable reduction in the intensity of the 2D band at 2686 cm^{-1} revealed an increase in the interlayer distance for rGO nanosheets, caused by the bulky polysaccharide molecules covalently attached to this nanomaterial.

This novel GC-rGO hybrid nanomaterial was further used as coating material for glassy carbon electrodes, and the resulting nanostructured surface was employed as scaffold for the covalent immobilization of the enzyme laccase through a glutaraldehyde-mediated cross-linking reaction. In this sense, we take advantage over the high content of hydroxyl and primary amino groups in the polysaccharide to form stable and multi-point covalent linkages between the enzyme molecule and the nanohybrid at the electrode surface. A noticeable smooth and homogeneous morphology was observed for the nanostructured surface after laccase immobilization, as revealed by FE-SEM analysis (Figure 1C), suggesting a high enzyme loading on the interface.

To employ this enzyme electrode as a biosensor for phenols determination, the conditions for the assembly of the Lac/GC-rGO/GCE electrode were optimized by evaluating the influence of different parameters on the amperometric signal for catechol. As can be observed in Figure 2S (Supporting Information), larger analytical responses were achieved by coating the electrodes with 12.5 µg of GC-rGO. Large nanohybrid loadings caused a decrease in the amperometric response which was ascribed to low mechanical stability of the resulting film, thus leading to leaking from the electrode surface. In addition, the enzyme electrode displayed maximum amperometric signals when 120 µg laccase were immobilized on the nanostructured electrode by using 0.5% (v/v) glutaraldehyde as cross-linking agent. Electrodes loaded with larger enzyme amounts yielded lower measured currents which could be attributed to the formation of non-conducting enzyme multi-layer assemblies, causing diffusional restriction of the substrate to the inner enzyme layers and also hindering the electron transfer properties at the electrode surface.

Electrochemical impedance spectroscopy (EIS) was employed to monitor the assembly of the enzyme electrode under the optimized conditions using $[Fe(CN)_6]^{4-/3-}$ as redox probe. All the experimental data were obtained by fitting with a conventional Randles equivalent circuit, and the resulting Nyquist plots are shown in Figure 3. As a control, the electrochemical impedance spectrum of a GCE coated with GO was also measured.

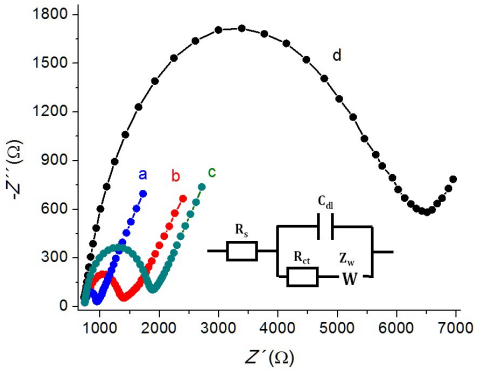

Figure 3. Impedance plane diagram (−Z″ versus Z′) for the EIS measurements at a GCE before (a) and after coating with GC-rGO (b), GO (c) and Lac/GC-rGO (d) in 0.1 M KCl solution containing 5 mM $K_3[Fe(CN)_6]/K_4[Fe(CN)_6]$ (1:1).

It was noticed that the electron transfer resistance (R_{et}) was increased from 420 to 1115 Ω after modification with the hybrid nanomaterial. Interestingly, a large increase in the R_{et} value of 1700 Ω was observed for the control electrode coated with GO. This fact suggests high conductivity properties for the nanohybrid, then favouring the fast occurrence of the electron transfer processes at the surface of the nanostructured electrode. Taking into account the non-conductive properties of the polysaccharide molecules in the hybrid nanomaterial, this result can be only justified by a partial recovery of the electroconductive properties of graphene after covalent grafting of glycol chitosan on Sil-GO, due to the mentioned reduction of the oxygen functional groups at the basal plane of GO. Similar transformation has been previously described for GO after treatment with primary amine compounds.[16,38] Covalent immobilization of laccase on GC-rGO/GCE caused a noticeable increase in the electron transfer resistance (R_{et} = 6860 Ω) due to the insulating effect of the protein molecules, thus indicating a high enzyme loading on the electrode interface.

View Article Online
DOI: 10.1039/C5AN02640G

Figure 4 shows the cyclic voltammetric response of the enzyme electrode toward catechol. As a control, a related electrode architecture without glycol chitosan (Lac/rGO/GCE) was also tested. A well-defined pair of redox peaks, corresponding to the quasi-reversible catechol/*o*-benzoquinone system at the electrode surface, was observed for the Lac/GC-rGO/GCE electrode. In addition, a remarkable larger peak potential separation and noticeable lower peak currents were apparent at the Lac/rGO/GCE control electrode. This fact suggests a larger loading of active enzyme on the electrode prepared with GC-rGO nanohybrid which is most likely due to the presence of primary amino groups at the polysaccharide chains allowing stable glutaraldehyde-mediated multi-point cross-linking with the ε-amino groups from lysine residues at the laccase surface. Moreover, hydrophilicity of glycol chitosan should favor keeping the active enzyme conformation on the electrode surface upon immobilization.

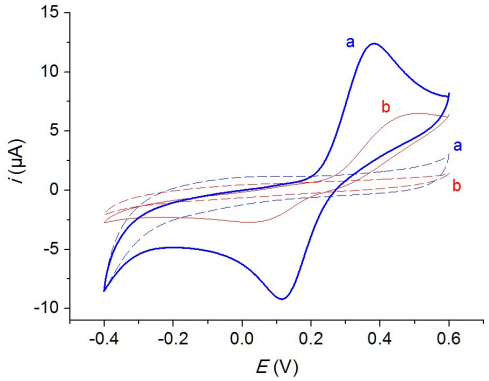

Figure 4. Cyclic voltammograms recorded at Lac/GC-rGO/GCE (a) and Lac/rGO/GCE (b) electrodes in in 0.1 M sodium phosphate buffer, pH 5.5 in the absence (dotted lines) and the presence (solid lines) of 60 μM catechol. Scan rate: 50 mV/s.

The operational conditions for the amperometric detection of phenols were optimized using catechol as analyte. As can be observed in Figure 3S (Supporting Information), higher amperometric signals were achieved when the working potential was fixed at -150 mV *vs* Ag/AgCl, and the electroanalytical measurements were performed at pH 5.5. Accordingly, these values were selected to carry out further experiments.

Table 1. Analytical performance of the Lac/GC-rGO/GCE biosensor for different phenolic compounds.

Compound	Linear Range (μM)	Sensitivity (mA/M)	r	LOD[a] (nM)
Cathecol	0.2 - 15	6.5	0.998	76
3,4-Xylenol	9.9 – 30	0.4	0.987	5000
Phenol	5 – 30	0.2	0.998	4900
Hydroquinone	5 – 30	2.0	0.999	2500
4-Cloro-1-naphtol	5 – 19	0.78	0.997	4300

[a] LOD: Limit of detection.

The Lac/GC-rGO/GCE enzyme electrode was tested for the quantification of several phenolic compounds able to behave as substrates for laccase. As an example, Figure 5 shows the amperometric responses of the biosensor upon continuous addition of catechol, and the resulting calibration curve. In addition, Table 1 summarizes the analytical characteristics of the corresponding calibration curves toward different phenolic compounds. Laccase is a polyphenol oxidase showing better catalytic performance toward diphenols than for mono-phenol substrates.[39] This is in agreement to the behavior observed with the developed enzyme biosensor toward catechol with respect to the other substrates checked.

The enzyme biosensor was able to detect phenol, 3,4-xylenol, hydroquinone and 4-cloro-1-naphtol at micromolar level, but best electroanalytical behaviour was observed toward catechol with a linear range of response from 200 nM to 15 μM (n = 10, r = 0.998), according to the following equation:

$$i_c(\text{mA}) = 6.5\times c(\text{catechol/M}) - 3.0\times10^{-6}$$

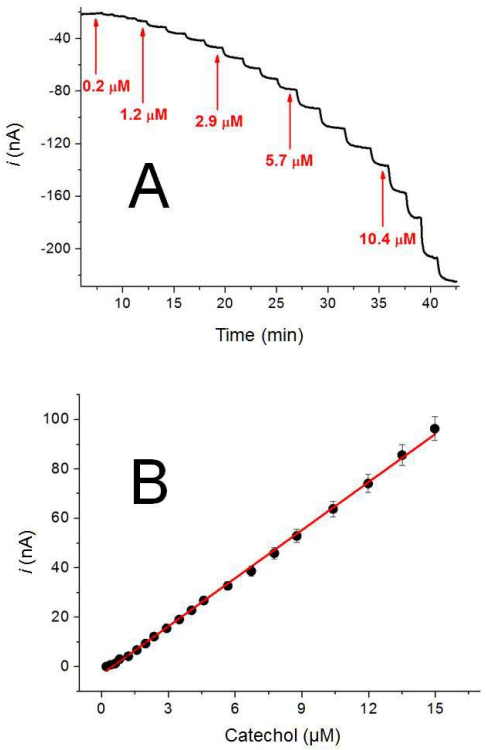

Figure 5. Amperometric responses (A) and calibration curve (B) obtained with the Lac/GC-rGO/GCE toward catechol. E_{app} = -150 mV.

The biosensor showed a fast analytical response, reaching 95% of the steady-state current within 7 seconds after the addition of catechol. The enzyme biosensor also showed a high sensitivity of 6.49 mA/M (93 mA/M cm^2) and a low detection limit of 76 nM, which was calculated according to the $3S_b/m$ criterion, where m is the slope of the calibration curve reported in Figure 5B and S_b was estimated as the standard deviation of 10 different electroanalytical signals recorded for the lowest catechol concentration measured in the calibration graph (200 nM).

The comparison of the electroanalytical behaviour of this enzyme electrode with respect to other previously reported laccase-based biosensors is made in Table 1S (Supporting Information). As can be observed, the Lac/GC-rGO/GCE biosensor showed broader linear range of response and lower detection limit than those reported for laccase electrodes involving multi-walled carbon nanotubes/chitosan composite on GCE (1.2 – 30 μM, 660 nM),[24] nitrogen-doped ordered mesoporous carbon/polyvinil alcohol film on gold electrode (0.39 – 8.98 μM, 310 nM),[25] polyaniline coated GCE (3.2 – 19.6 μM, 2.07 μM),[27] palladium-copper

View Article Online
DOI: 10.1039/C5AN02640G

alloyed nanocages/rGO nanohybrid on GCE (1.7 – 5.2 mM, 1.5 μM),[28] cysteamine-modified gold electrodes (10 – 100 μM, 4.8 μM),[30] and gold nanoparticles-modified zein ultrafine fibers/Nafion composite on GCE (0.17 – 7 μM, 166 nM).[33] On the other hand, the apparent kinetics constants for the enzyme-mediated catalytic transformation of catechol on the electrode surface were determined by means of the Lineweaver-Burk plots and the estimated values for K_M and I_{MAX}, were 93.4 μM and 500 nA, respectively.

The reproducibility of the amperometric measurements made with the laccase-based biosensor was assessed by performing successive additions of catechol in the 1.0 – 6.0 μM range. The R.S.D. value calculated from the slopes of the resulting calibration plots was 3.0% (n = 10). Moreover, the electrode-to-electrode reproducibility was evaluated by measuring the slope values of the calibration plots constructed with five different biosensors prepared in the same manner. The enzyme biosensor showed an excellent reproducibility, with an R.S.D. value of 4.1%.

The influence of several potential interfering compounds was evaluated by measuring the effect of these substances at 1 mM concentration on the amperometric response for 100 nM catechol. No significant effect was observed for D-glucose, fructose, D-galactose, NO_3^-, 17β-estradiol, 17α-ethinyl estradiol, bisphenol A and uric acid. However, an increase of about 17% in the cathodic current was observed in the presence of ascorbic acid, suggesting a significant interference of this compound.

The storage stability of the biosensor was tested at 4ºC under dry and wet conditions (50 mM sodium phosphate buffer, pH 5.5) by measuring its amperometric response toward 1.0 μM catechol over 3 weeks of storage. As can be observed in Figure 4S (Supplementary Information), the enzyme electrode exhibited excellent storage stability when storing in wet conditions, retained full catalytic activity after 15 days of storage. Longer storage periods caused a progressive decrease in the electroanalytical response of the electrode, according to first-order kinetics process, retaining about 42% of the initial activity after 3 weeks. On the contrary, the enzyme electrode showed a fast loose of electroanalytical performance when stored in dry conditions, retaining only 18% of the initial activity after one week of storage.

To confirm the suitability and potential application of the enzyme electrode for analytical purposes, the total phenolic compounds content (as catechol) in herbal tea samples was measured. The obtained results were compared with those provided by the conventional Folin-Ciocalteau colorimetric method for phenols,[37] using catechol as standard. As can be observed in Figure 5S (Supporting Information), the analytical signals obtained by both methods correlated linearly for all samples tested, suggesting this enzyme biosensor could be successfully employed as analytical tool to determine total phenol content in real samples. Accordingly, a total phenol content of 25 ± 2.8, 13 ± 2 and 15 ± 3 was estimated for red fruit tea, peppermint tea and green-lemon tea, respectively, by using the bioelectroanalytical method.

Furthermore, the enzyme electrode was tested for the simultaneous determination of catechol and 4-aminophenol, using differential pulse voltammetry (DPV). As can be observed in Figure 6A, the cathodic peak current increased linearly with catechol concentration in the 1.0 – 69 μM range, according to the following equation (r = 0.996):

$$i_c(\text{mA}) = 31.7\times c(\text{catechol/M}) + 3.7\times10^{-5}$$

with a limit of detection of 800 nM (S/N = 3) and a sensitivity of 454 mA/M cm^2.

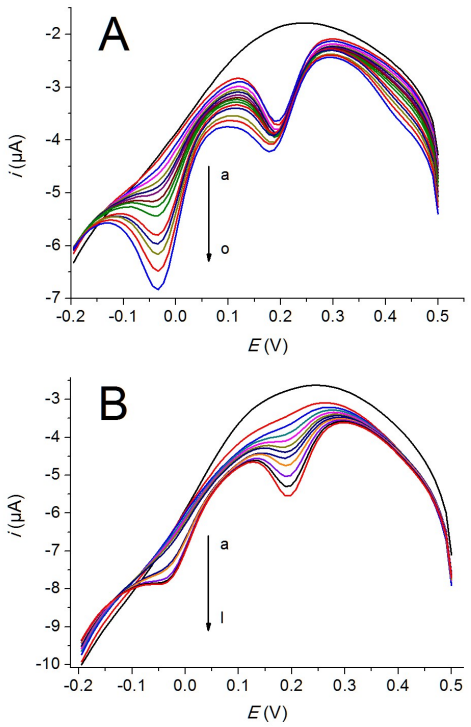

Figure 6. (A) Differential pulse voltammograms recorded with the Lac/GC-rGO/GCE in the presence of 20 μM 4-aminophenol containing different concentrations of catechol (a-o: 0, 1, 5, 10, 14, 18, 22, 25, 29, 33, 37, 40, 50, 58 and 69 μM). (B) Differential pulse voltammograms recorded with the Lac/GC-rGO/GCE in the presence of 40 μM catechol containing different concentrations of 4-aminophenol (a-l: 0, 0.5, 2, 3, 4, 5, 6, 10, 12, 16, 18 and 20 μM).

Also, Figure 6B shows as the biosensor exhibited similar electroanalytical behaviour toward 4-aminophenol, with a linear range of response from 500 nM to 20 μM (r = 0.995), according to the following equation:

$$i_c(\text{mA}) = 62.6\times c(\text{4-aminophenol/M}) + 3.2\times10^{-5}$$

The biosensor showed a sensitivity of 897 mA/M cm^2 and a detection limit of 310 nM (S/N = 3) for 4-aminophenol.

Conclusions

A novel water-soluble hybrid nanomaterial was prepared by covalent grafting glycol chitosan on the surface of graphene oxide. This nanohybrid was succesfully employed as coating material for glassy carbon electrodes to allow covalent and stable immobilization of the enzyme laccase. The nanostructured enzyme electrode exhibited excellent analytical performance toward catechol in terms of low limit of detection and high sensitivity and stability. Our results suggest that this novel graphene-based hybrid nanomaterial could be a valuable transducer element for the assembly of advanced electroanalytical devices to be employed in biosensing applications.

View Article Online
DOI: 10.1039/C5AN02640G

Acknowledgements

Financial support from the Spanish Ministry of Economy and Competitiveness CTQ2014-58989-P, CTQ2011-24355, CTQ2015-71936-REDT, CTQ2012-34238 and Comunidad de Madrid S2013/MIT-3029, Programme NANOAVANSENS is gratefully acknowledged.

Notes and references

[a]*Department of Analytical Chemistry &* [b]*Department of Organic Chemistry I, Faculty of Chemistry, Complutense University of Madrid, 28040-Madrid Spain.*
[c]*IMDEA Nanoscience, Ciudad Universitaria de Cantoblanco, 28049-Madrid, Spain.*
**Corresponding authors: Fax: +34 913944329; Tel: +34 913944315;*
E-mail: pingarro@quim.ucm.es, rvillalonga@quim.ucm.es.

†Electronic supplementary information (ESI) available: Optimization of biosensor construction and stability studies.

1 A. Cao, H. Ai, Y.Ding, C. Dai, and J. Fei, *Sensor Actuat B-Chem*, 2011, **155**(2), 632-638.
2 R. Villalonga, A. Fujii, H. Shinohara, Y. Asano, R. Cao, S. Tachibana, and P. Ortiz,. *Biotechnol. Lett*., 2007, **29**(3), 447-452.
3 A. Garcia, C. Peniche-Covas, B. Chico, B. K. Simpson, and R. Villalonga,. *Macromol. Biosci.*, 2007, **7**(4), 435-439.
4 M. Holzinger, A. Le Goff, and S. Cosnier, *Front. Chem*. 2014, **2**.
5 A. Walcarius, S. D. Minteer, J. Wang, Y. Lin and A. Merkoçi, *J. Mater. Chem. B*, 2013, **1**(38), 4878-4908.
6 R. Villalonga, P. Díez, S. Casado, M. Eguílaz, P. Yáñez-Sedeño and J. M. Pingarrón, *Analyst*, 2012, **137**(2), 342-348.
7 P. Díez, C. G. Piuleac, P. Martínez-Ruiz, S. Romano, M. Gamella, R. Villalonga and J. M. Pingarrón, *Anal. Bioanal. Chem.*, 2013, **405**(11), 3773-3781.
8 W. Zhang, A. M. Asiri, D. Liu, D. Du, and Y. Lin, *TrAC Trends Anal. Chem.*, 2014, **54**, 1-10.
9 Y. Song, Y. Luo, C. Zhu, H. Li, D. Du, and Y. Lin, *Biosens. Bioelectron.*, 2016, **76**, 195-212.
10 E. Araque, C. B. Arenas, M. Gamella, J. Reviejo, R. Villalonga, and J. M. Pingarrón, *J. Electroanal. Chem.*, 2014, **717**, 96-102.
11 F. H. Cincotto, T. C. Canevari, S. A. Machado, A. Sánchez, M. A. R. Barrio, R. Villalonga, and J. M. Pingarrón, *Electrochim. Acta*, 2015, **174**, 332-339.
12 T. Kuila, S. Bose, P. Khanra, A. K. Mishra, N. H. Kim and J. H. Lee, *Biosens. Bioelectron*., 2011, **26**(12), 4637-4648.
13 M.J. Allen, V.C. Tung, R.B. Kaner, Chem. Rev., 2010, **110**, 132-145.
14 Q. Fan, J. M. Gottfried and J. Zhu, *Accounts Chem. Res*., 2015, **48**(8), 2484-2494.
15 Y. Liu, X. Dong, P. Chen, *Chem. Soc. Rev*., 2012, **41**, 2283-2307.
16 E. Araque, R. Villalonga, M. Gamella, P. Martínez- Ruiz, J. Reviejo, and J. M. Pingarrón, *J. Mater. Chem. B*, 2013, **1**(17), 2289-2296.
17 A. Boujakhrout, A. Sánchez, P. Díez, S. Jiménez-Falcao, P. Martínez-Ruiz, M. Peña-Álvarez, J.M. Pingarron and R. Villalonga, *J. Mater. Chem. B*, 2015, **3**(17), 3518-3524.
18 B. Borisova, J. Ramos, P. Díez, A. Sánchez, C. Parrado, E. Araque, R. Villalonga, and J. M. Pingarrón, *Electroanal.*, 2015, **27**(9), 2131-2138.
19 W. Suginta, P. Khunkaewla and A. Schulte, *Chem. Rev.*, 2013, **113**(7), 5458-5479.
20 Y. Bo, W. Wang, J. Qi, and S. Huang, *Analyst*, 2011, **136**(9), 1946-1951.
21 Q. Zeng, J. S. Cheng, X. F. Liu, H. T. Bai, and J. H. Jiang, *Biosens. Bioelectron.*, 2011, **26**(8), 3456-3463.
22 L. Fernández, L. Gómez, H. L. Ramírez, M. L.Villalonga, and R. Villalonga, *J. Mol. Catal. B: Enzym.,* 2005, **34**(1), 14-17.
23 G. Gupta, V. Rajendran and P. Atanassov, *Electroanal.*, 2003, **15**(20), 1577-1583.
24 Y. Liu, X. Qu, H. Guo, H. Chen, B. Liu, and S. Dong, *Biosens. Bioelectron.*, 2006, **21**(12), 2195-2201.
25 M. Guo, H. Wang, D. Huang, Z. Han, Q. Li, X. Wang, and J. Chen, *Sci. Tech. Adv. Mater.*, 2014, **15**(3), 035005.
26 J. Qu, Y. Wang, J. Guo, T. Lou and Y. Dong, *Anal. Lett.,* 2014, **47**(15), 2537-2547.
27 M. Nazari, S. Kashanian, and R. Rafipour, *Spectrochim. Acta Mol. Biomol. Spectrosc.,* 2015, **145**, 130-138.
28 L. P.Mei, J. J. Feng, L. Wu, J. Y. Zhou, J. R. Chen and A. J. Wang, *Biosens. Bioelectron.*, 2015, **74**, 347-352.
29 S. Sadeghi, E. Fooladi and M. Malekaneh, *Appl. Biochem. Biotechnol.*, 2015, **175**(3), 1603-1616.
30 E. Akyilmaz, B. Şahin and H. Türkmen, *Sens Lett.*, 2014, **12**(10), 1519-1525.
31 J. Qu, T. Lou, S. Kang, and X. Du, *Sens Lett*, 2013, **11**(9), 1567-1572.
32 J. Qu, T. Lou, Y. Wang, Y. Dong, and H. Xing, *Anal. Lett.*, 2015, **48**(12), 1842-1853.
33 X. Chen, D. Li, G. Li, L. Luo, N. Ullah, Q. Wei, and F. Huang, *Appl. Surf. Sci.,* 2015, **328**, 444-452.
34 K. B. Pandey and S. I. Rizvi, *Oxid. Med. Cell Longev.,* 2009, **2**(5), 270-278.
35 Y. Cai, Q. Luo, M. Sun, and H. Corke, *Life Sci.*, 2004, **74**(17), 2157-2184.
36 S. Kitamura, T. Suzuki, S. Sanoh, R. Kohta, N. Jinno, K.Sugihara, S. Yoshihara, N. Fujimoto, H. Watanabe, and S. Ohta, *Toxicol. Sci.*, 2005, **84**(2), 249-259.
37 E. A. Ainsworth and K. M. Gillespie, *Nat. Protoc.,* 2007, **2**(4), 875-877.
38 L. Q. Xu, W. J. Yang, K. G. Neoh, E. T. Kang, and G. D. Fu, *Macromolecules*, 2010, **43**(20), 8336-8339.
39 C. F. Thurston, *Microbiology*, 1994, **140**, 19-26.
40 Z. Liu, Z. Wang, Y. Cao, Y. Jing, and Y. Liu, *Sensor Actuat B-Chem*, 2011, **157**(2), 540-546.

View Article Online
DOI: 10.1039/C5AN02640G

A sensitive laccase biosensor for phenols based on novel graphene oxide-glycol chitosan nanohybrid

View Article Online
DOI: 10.1039/C5AN02640G

Figure for Graphical Abstract
123x98mm (120 x 120 DPI)